Geophysical Research Letters

RESEARCH LETTER
10.1029/2022GL102145

This article is a companion to Wang et al. (2023), https://doi.org/10.1029/2023GL103719.

Key Points:

- At weekly to monthly forecast ranges, regional polar low (PL) activity is skillfully predicted using a PL genesis potential index
- Major climate modes can strongly influence regional prediction skill and can be used to identify forecasts of opportunity

Supporting Information:

Supporting Information may be found in the online version of this article.

Correspondence to:

Z. Wang,
zhuowang@illinois.edu

Citation:

Boyd, K., Wang, Z., Walsh, J., & Stoll, P. (2023). Subseasonal predictions of polar low activity using a hybrid statistical-dynamical approach. *Geophysical Research Letters*, *50*, e2022GL102145. https://doi.org/10.1029/2022GL102145

Received 16 NOV 2022
Accepted 6 MAY 2023

Subseasonal Predictions of Polar Low Activity Using a Hybrid Statistical-Dynamical Approach

Kevin Boyd[1], Zhuo Wang[1], John Walsh[2], and Patrick Stoll[3]

[1]University of Illinois at Urbana-Champaign, Urbana, IL, USA, [2]University of Alaska Fairbanks, Fairbanks, AK, USA, [3]Department of Physics and Technology, Arctic University of Norway, Tromsø, Norway

Abstract The subseasonal prediction of polar low (PL) activity is explored using a hybrid statistical-dynamical approach. A previously developed PL genesis potential index is paired with ECMWF reforecasts and forecasts to predict regional statistics of PL activity across the sub-Arctic. Regional PL activity is skillfully predicted in all regions at forecast ranges of up to a month. Additionally, the predictability limit of this hybrid framework (estimated using reanalysis data) is found to be highest over the Nordic Seas, Irminger Sea, Labrador Sea, and Bering Sea. We find that climate modes can strongly influence subseasonal prediction skill and are a potential source of predictability. Overall, our results highlight a promising prospect for the subseasonal prediction of PL activity.

Plain Language Summary Polar lows (PLs) are intense mesocyclones forming over high-latitude oceanic regions that pose hazardous risks to coastal communities and marine and air operations. This motivates the skillful prediction of PLs, which remains a major challenge at lead times beyond several days. We show that skillful forecasts of PL activity over a forecast range of weeks to a month in advance can be achieved by using a statistical modeling approach in combination with numerical model forecasts. Prediction skill varies by region, and is shown to be sensitive to major modes of variability in the large-scale atmospheric circulation.

1. Introduction

Polar lows (PLs) are intense maritime mesocyclones that occur during the winter season over high-latitude oceans (Rasmussen & Turner, 2003) with average horizontal length scales on the order of 300 km and lifetimes around 20 hr (Stoll, 2022). PLs can serve as major threats to human life and property through their associated severe weather conditions, such as gale-force winds, large-amplitude oceanic waves (Rojo et al., 2019), and heavy snowfall (Harrold & Browning, 1969). This motivates the skillful prediction of PL activity at short to extended lead times.

Forecasting PLs is a challenging task because PLs are short-lived mesoscale systems that develop quickly in sparsely observed oceans (Moreno-Ibáñez et al., 2021). Our short-term prediction capabilities have increased substantially in recent decades, with skillful predictions of storm track and intensity now being realized several days ahead (Müller et al., 2017; Stoll et al., 2020). On the other hand, PL predictability on the subseasonal time scale is yet to be studied, and subseasonal forecasts of PL activity are seldom issued, if at all. The subseasonal variability of PL activity has received some attention and been linked to certain modes of climate variability, including the Madden-Julian Oscillation (MJO; Wang et al., 2023), North Atlantic Oscillation (NAO; Claud et al., 2007; Mallet et al., 2013), Arctic Oscillation (AO; Boyd et al., 2022), and the Pacific North-American pattern (PNA; Chen & von Storch, 2013; Boyd et al., 2022), through the impacts of large-scale environmental conditions. These modes could serve as a source of subseasonal predictability for PL activity (or statistics of PLs, in contrast to individual PLs) and facilitate extended-range forecasts. Aside from densely populated coastal communities, such forecasts may be of great value to governments and stakeholders engaging in maritime transport in the Arctic, as the northward retreat of the sea ice has resulted in a proliferation in maritime transport that is projected to continue rising as the Arctic becomes increasingly more navigable (Smith & Stephenson, 2013).

The prediction of PLs on the subseasonal time scale is complicated by their small spatio-temporal scales, which are often insufficiently resolved by coarse-resolution global models (Zappa et al., 2014). One solution is to utilize empirical relationships between storm frequency and large-scale climate conditions, an approach that has been applied considerably to tropical cyclone prediction (e.g., Klotzbach et al., 2019) and tornado prediction (Miller et al., 2020). A PL genesis potential index (PGI) has been developed for PLs (Boyd et al., 2022). It

utilizes static stability and environmental baroclinicity as climate predictors and is able to skillfully capture the observed seasonality, spatial distribution, and interannual variability of PL activity across the sub-Arctic domain. This study will demonstrate that skillful subseasonal prediction of PL activity can be achieved using the PGI in a hybrid statistical-dynamical approach resembling an operational forecasting scenario. In addition, we will explore the predictability limit of this hybrid framework and examine how predictability varies by region, forecast range, and climate state.

2. Data and Methodology

2.1. PL Track Data Set and PL Genesis Potential Index

We use the PL data set developed by Stoll (2022), which contains tracks for 13,888 PLs in the Northern Hemisphere. The data set was obtained by selecting mesoscale cyclone tracks (Watanabe et al., 2016) that satisfy observationally-based PL identification criteria (PL-IC; Stoll, 2022). We identify the locations of PL genesis as the first instance in a PL track when all PL-IC are satisfied simultaneously (with an additional distance-to-land requirement of 75 km, which disqualifies 2,911 PL tracks) and interpolate them to the nearest 2.5° × 2.5° grid cell to get the PL genesis density function.

Predictions of PL activity are carried out using the PGI, which is a log-linear function that relates two standardized, large-scale climate predictors, static stability (S) and environmental baroclinicity (B), to PL genesis frequency:

$$\log PGI = b + b_S S + b_B B + \log\cos\varphi \quad (1)$$

where φ is the latitude; b, b_S, and b_B represent regression coefficients (see more information in Section 2.2). S and B are, respectively, the potential temperature difference between the surface and 500 hPa, and the magnitude of the horizontal gradient of the equivalent potential temperature (θ_e) at 800 hPa. Due to data availability limitations, the B predictor will instead be based on the 850-hPa level.

2.2. Prediction of PL Activity

We predict weekly and monthly PL genesis frequency using the PGI in tandem with dynamical forecasts from two closely-related forecasting systems available from the European Centre for Medium-Range Weather Forecasts (ECMWF). Weekly prediction utilizes the climate predictors (S and B) derived from the ECMWF operational extended-range forecasting system (Vitart et al., 2017, 2019), hereafter referred to as the weekly prediction model (WPM). We consider forecast ranges of week 1 (Day 1–7), week 2 (Day 8–15), and weeks 3 and 4 (Day 16–30). Monthly prediction (forecast range of Day 1–31) employs the ECMWF operational seasonal forecasting model, the SEAS5 (Johnson et al., 2019). Predictors derived from the ECMWF forecasting models are interpolated to a common 2.5° × 2.5° grid resolution.

The temporal domain of our analysis is determined by the availability of reforecasts and forecasts; it ranges from 1993 to 2020 for monthly prediction, and from 1995 to 2020 for weekly prediction. We focus on the PL season (November–March) during these time periods. The WPM has a reforecast ensemble size ranging from 5–11 depending on the model version, while the SEAS5 has a 25-member ensemble for its reforecasts. For both models, the ensemble size for forecasts is 51. Across ensemble members, a total of 12,036 (1020) forecasts and 52,020 (3000) reforecasts are extracted from the WPM (SEAS5).

Monthly prediction is carried out using a leave-one-out cross-validation approach (Wilks, 2011), where the ensemble reforecasts or forecasts from one PL season is left out as the testing data set and the ensemble-mean reforecasts and forecasts from the remaining years serve as the training data set. This is repeated for each year, yielding a time series of the predicted PL frequency. For weekly prediction, the training data set consists of the ensemble-mean reforecasts initialized prior to 01 January 2015 (the beginning of the forecast period), while the ensemble of forecasts and all remaining reforecasts (initialized after 01 January 2015) comprise the testing data set.

The regional statistics (areal mean of climate predictors and areal sum of PL genesis frequency) are computed for specific regions (Figure S1 in Supporting Information S1). For each region and forecast range, the Poisson

regression model is fit to the corresponding time-averaged regional statistics (with predictors standardized) to determine the regression coefficients. PGI predictions are then executed for each ensemble member in the testing data set, yielding ensemble PGI predictions. To estimate the upper limit of prediction skill of the hybrid framework, the climate predictors (S and B) derived from ERA5 reanalysis (Hersbach et al., 2020) are utilized as truth by matching the output characteristics (time period and spatio-temporal resolution) of both ECMWF forecasting models. The procedure for model training and evaluation is identical, except the reanalysis does not feature an ensemble.

2.3. Evaluation of Prediction Skill

Our evaluation of prediction skill will be focused on the mean of ensemble PGI predictions, while the ensemble spread is used to assess uncertainty. The anomaly correlation coefficient (or Pearson correlation; hereafter, ACC), root-mean-square error (RMSE), and Heidke skill score (HSS) serve as metrics for the evaluation of prediction skill. To compute the HSS, we adopt a 2-tier categorization system, with anomalies (based on weekly or monthly climatology) above or below zero. HSS values greater than zero are considered to be more skillful than the reference forecast (random forecasts; Wilks, 2011).

The impacts of climate modes on prediction skill are investigated. We utilize monthly mean climate indices to examine the impacts of the NAO, AO, PNA, and El Niño-Southern Oscillation (ENSO) on monthly prediction skill during the forecast validation time. The positive, negative, and neutral phases of these modes is defined by a threshold of ± 0.5 on the corresponding normalized climate index. For weekly predictions, we focus on the MJO and utilize the daily real-time multivariate MJO (RMM) indices (Wheeler & Hendon, 2004) to categorize initialization dates by MJO phase. We employ a Monte Carlo resampling approach (based on 1,000 random samples) to assess the statistical significance of changes in prediction skill associated with each climate mode with respect to the corresponding neutral or inactive phase. More details regarding the characteristics of the data sets, model fitting, prediction, and evaluation can be found in the Supporting Information S1.

3. Subseasonal Prediction Skill and Predictability of PL Activity

The prediction skill and predictability of PL activity on the subseasonal time scale are assessed in this section. To discern the subseasonal predictability limit of PL activity, we draw inspiration from the definitions of intrinsic and practical predictability provided by Lorenz (2006). Intrinsic predictability, hereafter referred to as potential skill, is inferred from prediction using climate predictors derived from the ERA5 reanalysis. It represents a hypothetical situation in which the forecasting model perfectly reproduces the "observed" climate predictors, thus potential skill is solely determined by the strength of the relationship between the climate predictors and PL activity. On the other hand, predictions based on the ECMWF models represent practical prediction, where the prediction skill of climate predictors affects the skill of PL prediction, in addition to the predictor-PL relationship elaborated above.

3.1. Practical Prediction Skill

The predicted monthly mean PGI anomalies are plotted alongside the observed PL genesis frequency anomalies for each region in Figure 1. The observed time series show that PL genesis frequency exhibits large intraseasonal and interannual variability. While the mean of ensemble predictions tend to underestimate the observed variance (Table S1 in Supporting Information S1), the ACC is statistically significant (99% confidence) over all regions. The observed time series often lies within the ensemble envelope, except when the observed anomalies are especially strong. It is interesting to note that the prediction skill differs widely across the sub-Arctic. The maximum ACC (0.60) is found over the Bering Sea (Figure 1e), where the hybrid prediction captures about 35% of the observed variance, while the minimum ACC (0.29) is found over the Labrador Sea.

The HSS for regional predictions of monthly and weekly PL activity based on the ECMWF forecasting models is plotted in Figure 2. The regional ranking of monthly prediction skill assessed using the HSS (Figure 2a) and ACC (Figure 1) is largely consistent despite these metrics representing two different aspects of prediction skill. This indicates that our assessment of prediction skill is robust. For 1-week outlooks, the practical skill is between 30% and 55% (Figure 2b), but the rate of decrease in prediction skill during the following weeks varies widely. After 1-week outlooks, the Nordic Seas and Labrador Sea feature a sharp reduction in skill (Figures 2c and 2d). On the other hand, the prediction skill does not decline as much over the Bering Sea, Sea of Okhotsk, and Sea of Japan. We expect that these regions draw more information from low-frequency predictability sources, which will

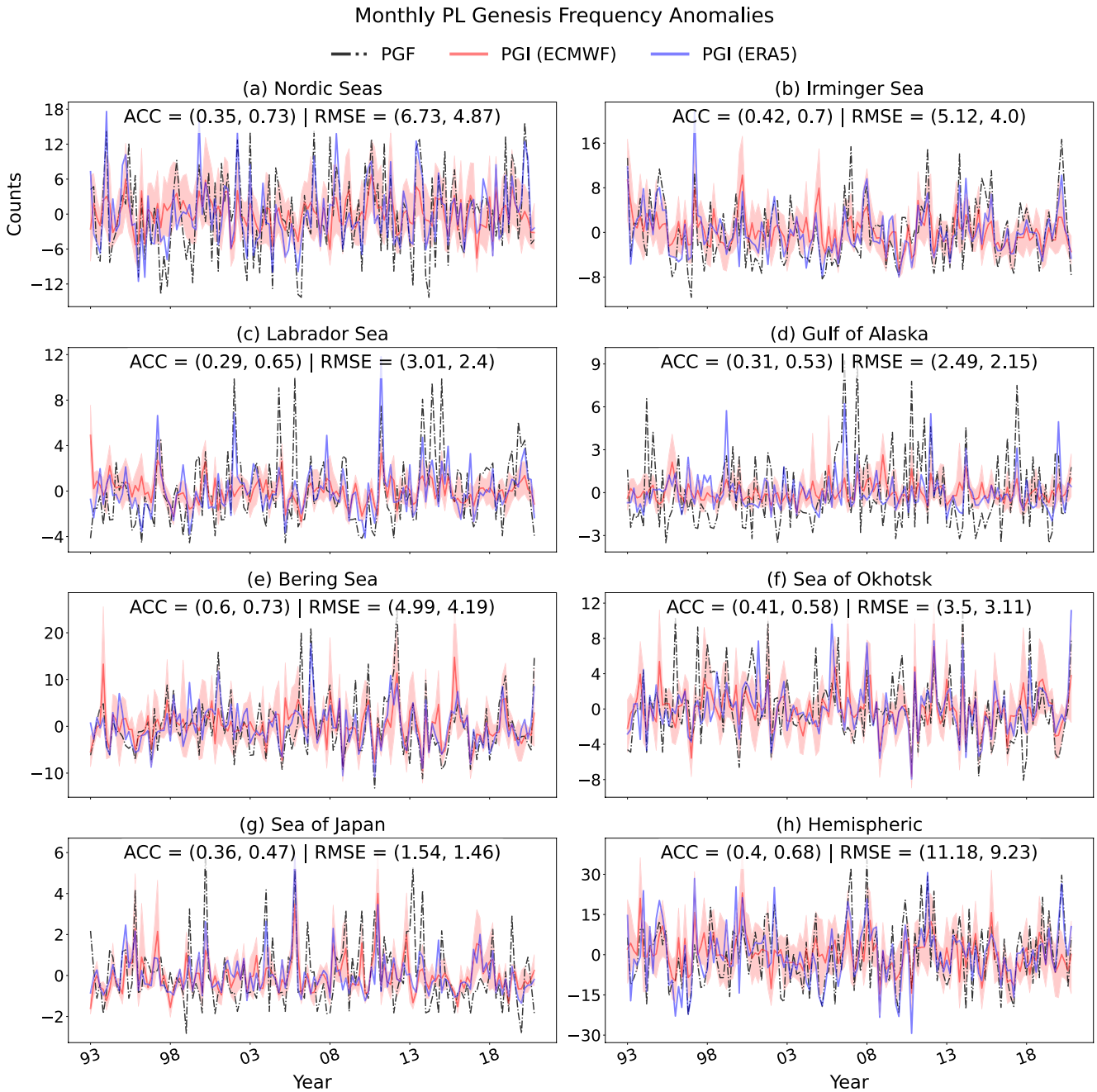

Figure 1. The monthly mean anomalies of observed polar low (PL) genesis frequency (dot-dashed lines) and PL genesis potential index (PGI) (predicted) time series from 1993 to 2020 for individual source regions (a–g) and the broader hemispheric domain (h). The anomaly correlation coefficient and root-mean-square error between the observed PL genesis frequency and PGI are shown in each panel title, with the first and second number in parenthesis representing predictions based on the SEAS5 model (red lines) and ERA5 reanalysis (blue lines), respectively. The 10th and 90th percentile of ensemble predictions is shown by the red shading.

be explored more in Section 4. Lastly, the HSS computed from the mean of ensemble PGI predictions typically surpasses the 90th percentile of ensemble HSS. The ensemble spread grows with increasing lead time and is largest for monthly-outlook predictions, indicating large prediction uncertainties.

3.2. Potential Prediction Skill

The PGI time series based on climate predictors derived from the ERA5 reanalysis are shown as blue curves in Figure 1, and the HSS for the "perfect" predictions is shown in hatched bars in Figure 2. The weekly to monthly

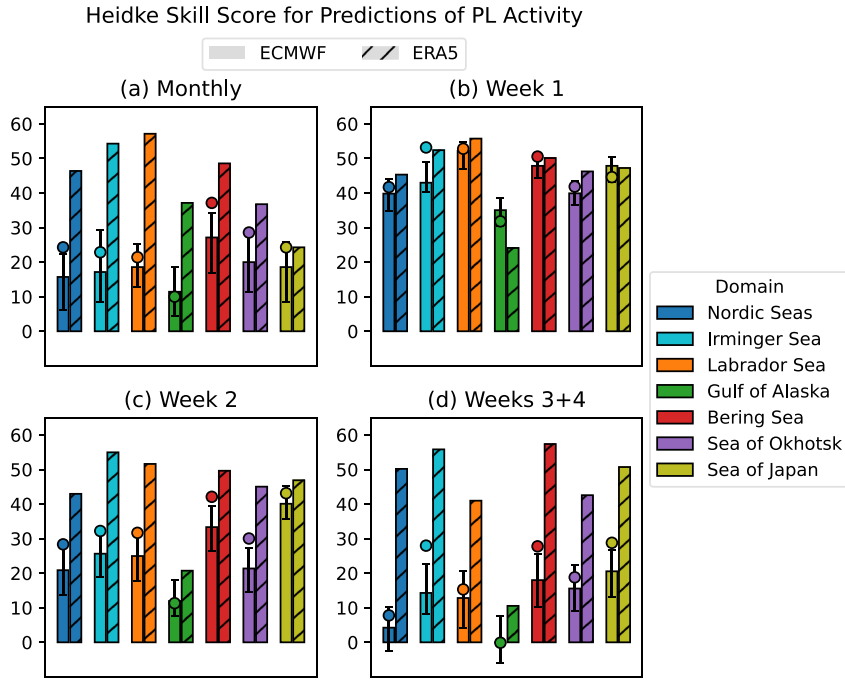

Figure 2. Heidke skill score (HSS) for regional predictions of monthly (a) and weekly (b–d) polar low (PL) activity based on the ECMWF forecasting models (solid) and ERA5 reanalysis (hatched). The solid bars represent the median HSS computed from ensemble PL genesis potential index (PGI) predictions, with accompanying error bars extending to the 10th and 90th percentile. The circular markers represent the HSS computed from the mean of ensemble PGI predictions.

potential prediction skill of regional PL activity varies across different regions, with the ACC ranging from 0.47 to 0.73 for monthly prediction (Figures 1a–1g) and a HSS around 30%–60% for weekly to monthly prediction (Figures 2a–2d). At the high end of ACC, such as over the Nordic Seas and Bering Sea, the PGI captures about 50% of the variance of PL activity. The lowest ACCs occur over the Sea of Japan and Gulf of Alaska. Overall, the analysis suggests potential predictability of PL activity on the subseasonal time scale in different regions.

The regional variations of potential prediction skill indicates that the strength of the predictor-PL relationship has a regional dependence. However, the difference between practical and potential prediction skill also varies strongly from region to region, indicating that the dynamical prediction skill of the climate predictors also has a regional dependence. This is exemplified by the large difference in practical ACC between the Nordic Seas (Figure 1a) and Bering Sea (Figure 1e) despite these regions having an identical potential ACC, which reflects the relatively poor prediction of the climate predictors by the SEAS5 over the Nordic Seas. The close relationship between practical and potential skill at lead times of up to 2 weeks (Figures 2b and 2c) indicates that the climate predictors are well forecasted on short forecast ranges. In general, the potential skill is greater than the practical skill over all forecast ranges and regions, but this is not the case over the Gulf of Alaska at 1-week outlook. We speculate that the tendency for synoptic-scale activity over this region (Chang et al., 2002) may be advantageous for the ECMWF-based predictions, due in part to the smoothing provided by the use of ensemble-mean predictors for model fitting.

4. Impacts of Climate Modes

We will assess the impacts of the AO, NAO, PNA, ENSO on the monthly prediction skill of PL activity in Section 4.1 and the impacts of the MJO on the weekly prediction skill of PL activity in Section 4.2. The degree to which a climate mode influences the prediction skill is dependent on (a) whether such mode (and phase) modulates the climate predictors, (b) the ability of the forecasting model to predict the future state of the mode and capture its imprint on the climate predictors, and (c) how well the PGI represents the impacts of the mode on PL activity. Our treatment will focus on how each climate mode affects prediction skill relative to the inactive or neutral phase.

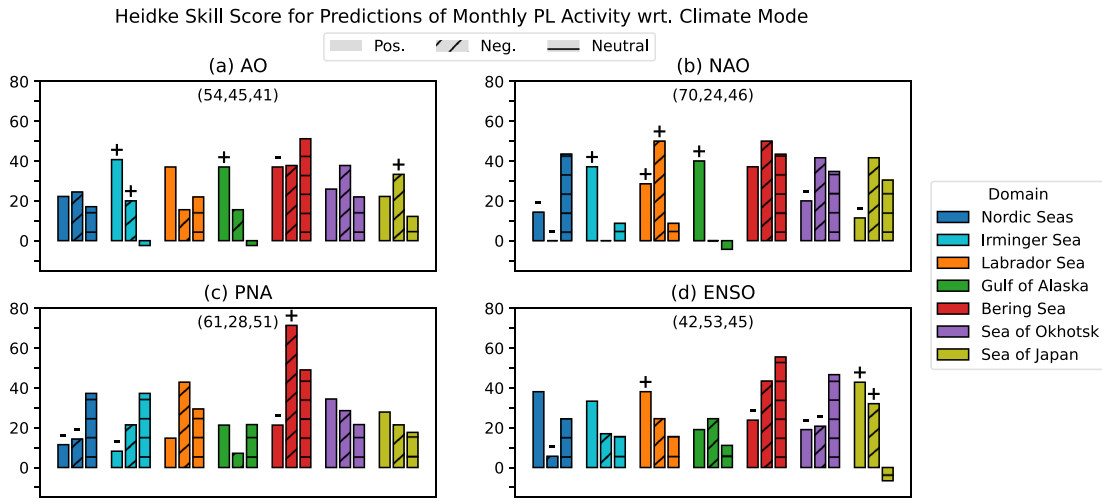

Figure 3. Heidke skill score for regional predictions of monthly polar low activity based on the SEAS5 model, separated by positive (solid), negative (hatched), and neutral (striped) phases of climate modes. In this respective order, the number of reforecast/forecast periods included in our analysis is indicated in parenthesis at the top of each panel. Skill scores greater (less) than the neutral skill with at least 90% significance are indicated with a "+" ("−").

4.1. Influence of the AO, NAO, PNA, and ENSO on Monthly Prediction Skill

The monthly prediction skill decomposed by climate modes, including the AO, NAO, PNA, and ENSO, is shown in Figure 3. The AO+ (AO−) phase is associated with enhanced (suppressed) PL activity over the West Atlantic through promotion (suppression) of favorable conditions, such as decreased (increased) static stability throughout the region, and a similar relationship also holds for the NAO (Boyd et al., 2022). We find significantly increased prediction skill over the Irminger Sea during the AO+ and AO− phases, but little impacts are present over the Labrador Sea. In contrast, the NAO+ and NAO− phases are associated with a significant enhancement of prediction skill over the Labrador Sea, while this only holds for the NAO+ phase over the Irminger Sea. The observed relationships between the AO/NAO and PL activity are skillfully represented by the PGI (Boyd et al., 2022), which suggests that the ECMWF model may sometimes struggle to capture the impacts of the AO and NAO over the West Atlantic. Over the Nordic Seas, we find that poor skill during the NAO likely represents a limitation of the PGI, as it tends to overestimate the impacts of the NAO over this region (Boyd et al., 2022). This may explain the rapid decrease in prediction skill with increasing forecast range over the Nordic Seas (Figure 2d). Interestingly, our findings also show that prediction skill over the Gulf of Alaska is significantly improved during the AO+ and NAO+ phases. The relationship between the AO/NAO and PL activity over the Gulf of Alaska is presently undocumented, and our findings might warrant a more detailed inquiry into these relationships.

Previous studies have noted a relationship between the PNA and PL activity over the central Pacific (Boyd et al., 2022; Chen & von Storch, 2013). Accordingly, the PNA has strong impacts on prediction skill over the Bering Sea (Figure 3c). We find that prediction skill is significantly increased (decreased) during the negative (positive) phase. Upon further investigation, there is considerably more variability in PL activity during the PNA+ phase in comparison to the PNA− phase, as the latter is generally associated with negative anomalies (Figure S2 in Supporting Information S1). The PGI predictions "expect" consistently positive anomalies during the PNA+ (a mirror opposite of the PNA–), and thus, struggle to capture its variability.

The impacts of ENSO on PL activity are weak across the sub-Arctic (Boyd et al., 2022), with the exception of the Sea of Okhotsk (Chen & von Storch, 2013). Over this region, the ENSO contributes to significantly decreased prediction skill in both phases. Evaluation against ERA5 suggests that the PGI struggles to represent the impacts of ENSO over the Sea of Oksotsk (not shown). Over the Sea of Japan, ENSO serves as a strong source of predictability, with significant improvements in prediction skill during both the positive and negative phase.

4.2. Impacts of the MJO on Weekly Prediction Skill

The MJO is a dominant mode of subseasonal variability in the Tropical Pacific (Madden & Julian, 1972) that has predictable influences on global weather patterns (Ferranti et al., 1990; Higgins et al., 2000; Jones et al., 2004), including links to the evolution and predictability of environmental conditions in the Arctic (Jung et al., 2016;

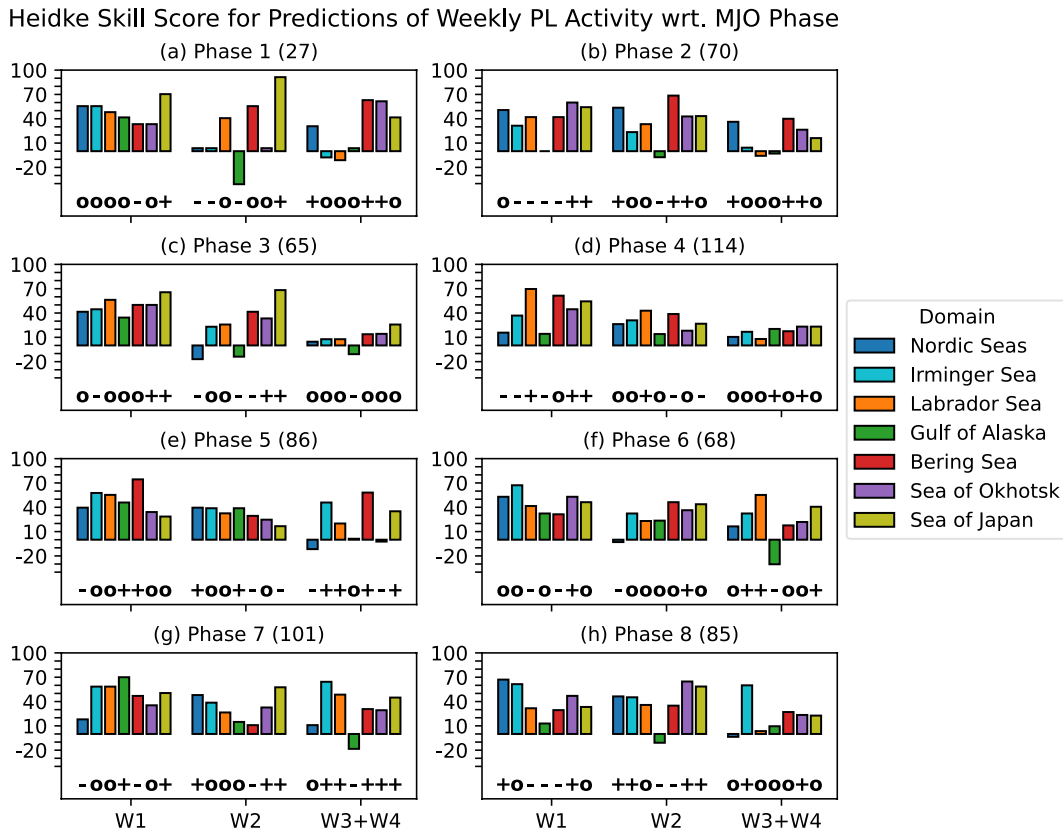

Figure 4. Heidke skill score for regional predictions of weekly polar low activity at forecast ranges of Day 1–7 (W1), Day 8–15 (W2), and Day 16–30 (W3 + W4) following an Madden-Julian Oscillation (MJO) event. The panel title indicates the MJO phase, alongside the corresponding number of reforecast/forecast periods included in our analysis. Skill scores greater (less) than the inactive phase ($|RMM| < 1$) with at least 90% significance are indicated with a "+" ("−") at the bottom of the figure panel, and insignificant skill scores are indicated with "o."

Lin, 2020). Wang et al. (2023) recently found that the MJO has strong impacts on PL activity across the sub-Arctic through the modulation of regional environmental conditions, and the PGI was able to skillfully represent these impacts. In the following paragraph, we will briefly explore how the MJO influences PL prediction skill.

The weekly prediction skill decomposed by MJO phases is shown in Figure 4. We find that the MJO can strongly influence subseasonal prediction skill, depending on the MJO phase and forecast range. We find several extraordinary examples where the HSS exceeds or nears 70% at week-1 forecast range, such as over the Bering Sea during phase 5, the Labrador Sea during phase 4, the Nordic Seas during phase 8, and the Gulf of Alaska during phase 7. These particular examples are associated with strong PL genesis frequency anomalies (see Fig. 1 in Wang et al., 2023), illustrating the predictable influences of the MJO on PL activity. Beyond the week-1 forecast range, significant large HSS values can be found over various regions depending on MJO phase, such as during phase 2 over the Bering Sea or during phase 1 over the Sea of Japan, where the HSS varies from 70% to over 90%. On the other hand, strong impacts of the MJO on PL activity do not always translate into enhanced prediction skill. An example is found over the Irminger Sea during phases 2–4 at week-1 and week-2 forecast range, where strong PL genesis frequency anomalies are represented by the PGI derived from the ERA5 (Figures 1n and 4n in Wang et al., 2023), suggesting that the WPM is sometimes unable to capture the extratropical impacts of the MJO on the regional climate conditions, which leads to poor PL prediction. It is important to note that our limited sample size may introduce sample fluctuations, so the influence of the MJO on PL prediction skill could be worth revisiting on a larger scale in future studies.

5. Summary and Outlook

The subseasonal prediction and predictability of PL activity is explored, for the first time as far as we are aware, for several regions across the sub-Arctic by utilizing the PGI (Boyd et al., 2022) paired with ECMWF forecasting

models and ERA5 reanalysis. The PGI relates regional statistics of PL activity with large-scale environmental conditions (i.e., static stability and environmental baroclinicity). Predictions are trained and evaluated against a PL data set using the HSS, Pearson correlation, and root-mean-square error. The impacts of climate modes, including the AO, NAO, PNA, ENSO, and MJO, are examined as well. Our primary findings are as follows:

- The weekly to monthly anomalies of PL activity are skillfully predicted (relative to random forecasts) over all regions (Figure 2), of which the Bering Sea is the best performing. The week-1 practical prediction skill is close to the potential prediction skill (Figure 2b) for all regions. In subsequent weeks (Figures 2c and 2d), the prediction skill drops sharply over the Labrador Sea and Nordic Seas but does not decline as much over the Bering Sea, Sea of Okhotsk, and Sea of Japan.
- The potential prediction skill indicates predictability of PL activity using the PGI. In particular, predictability is highest over the Nordic Seas, Irminger Sea, Labrador Sea, and Bering Sea (Figures 1 and 2), where the weekly or monthly HSS for potential prediction can reach up to 60%. However, large differences between practical and potential skill can be present due to the poor dynamical prediction of the climate predictors over certain regions.
- Climate modes can be used to identify forecasts of opportunity (Figures 3 and 4), but the impacts of a climate mode on PL prediction strongly depends on how skillfully the climate mode and the associated teleconnection are predicted.

We show that the prospects for the subseasonal prediction of PL activity are promising, and we do so with hopes that extended lead times will increase opportunities for planning and mitigation actions during periods of heightened risk of PLs.

Data Availability Statement

The ERA5 reanalysis is made available via the Research Data Archive (RDA) by the NCAR CISL https://rda.ucar.edu/datasets/ds633.0/. The polar low track data set is made available by Dr. Patrick Stoll at https://doi.org/10.18710/TVZDBF. Data from the ECMWF's operational extended-range forecasting model are extracted from the S2S database hosted at ECMWF (https://apps.ecmwf.int/datasets/data/s2s). Data from the ECMWF's SEAS5 model is available via the Climate Data Store (https://cds.climate.copernicus.eu/cdsapp#!/dataset/10.24381/cds.68dd14c3). The AO, NAO, PNA, and ENSO indices can be downloaded from the Climate Prediction Center (CPC) at https://www.cpc.ncep.noaa.gov/products/precip/CWlink/. The RMM indices are made available by the Australian Bureau of Meteorology at http://www.bom.gov.au/climate/mjo/.

Acknowledgments
This study was supported by the Office of Naval Research through Grant N000141812216. We acknowledge the National Center for Atmospheric Research (NCAR) Computational and Information Systems Laboratory (CISL) for providing computing resources and access to the ERA5 reanalysis. This work is based on S2S data. S2S is a joint initiative of the World Weather Research Programme (WWRP) and the World Climate Research Programme (WCRP).

References

Boyd, K., Wang, Z., & Walsh, J. E. (2022). A genesis potential index for polar lows. *Journal of Climate*, *35*(24), 7891–7902. https://doi.org/10.1175/jcli-d-22-0100.1

Chang, E. K. M., Lee, S., & Swanson, K. L. (2002). Storm track dynamics. *Journal of Climate*, *15*(16), 2163–2183. https://doi.org/10.1175/1520-0442(2002)015<02163:std>2.0.co;2

Chen, F., & von Storch, H. (2013). Trends and variability of North Pacific polar lows. *Advances in Meteorology*, *2013*, 170387. https://doi.org/10.1155/2013/170387

Claud, C., Duchiron, B., & Terray, P. (2007). Associations between large-scale atmospheric circulation and polar low developments over the North Atlantic during winter. *Journal of Geophysical Research*, *112*(D12), D12101. https://doi.org/10.1029/2006jd008251

Ferranti, L., Palmer, T. N., Molteni, F., & Klinker, E. (1990). Tropical-extratropical interaction associated with the 30–60 day oscillation and its impact on medium and extended range prediction. *Journal of the Atmospheric Sciences*, *47*(18), 2177–2199. https://doi.org/10.1175/1520-0469(1990)047<2177:teiawt>2.0.co;2

Harrold, T. W., & Browning, K. A. (1969). The polar low as a baroclinic disturbance. *Quarterly Journal of the Royal Meteorological Society*, *95*(406), 710–723. https://doi.org/10.1002/qj.49709540605

Hersbach, H., Bell, B., Berrisford, P., Hirahara, S., Horányi, A., Muñoz-Sabater, J., et al. (2020). The ERA5 global reanalysis. *Quarterly Journal of the Royal Meteorological Society*, *146*(730), 1999–2049. https://doi.org/10.1002/qj.3803

Higgins, R. W., Schemm, J. E., Shi, W., & Leetmaa, A. (2000). Extreme precipitation events in the western United States related to tropical forcing. *Journal of Climate*, *13*(4), 793–820. https://doi.org/10.1175/1520-0442(2000)013<0793:epeitw>2.0.co;2

Johnson, S. J., Stockdale, T. N., Ferranti, L., Balmaseda, M. A., Molteni, F., Magnusson, L., et al. (2019). SEAS5: The new ECMWF seasonal forecast system. *Geoscientific Model Development*, *12*(3), 1087–1117. https://doi.org/10.5194/gmd-12-1087-2019

Jones, C., Waliser, D. E., Lau, K. M., & Stern, W. (2004). Global occurrences of extreme precipitation and the Madden-Julian Oscillation: Observations and predictability. *Journal of Climate*, *17*(23), 4575–4589. https://doi.org/10.1175/3238.1

Jung, T., Gordon, N. D., Bauer, P., Bromwich, D. H., Chevallier, M., Day, J. J., et al. (2016). Advancing polar prediction capability on daily to seasonal time scales. *Bulletin of the American Meteorological Society*, *97*(9), 1631–1647. https://doi.org/10.1175/bams-d-14-00246.1

Klotzbach, P., Blake, E., Camp, J., Caron, L., Chan, J., Kang, N., et al. (2019). Seasonal tropical cyclone forecasting. *Tropical Cyclone Research and Review*, *8*(3), 134–149. https://doi.org/10.1016/j.tcrr.2019.10.003

Lin, H. (2020). Subseasonal forecast skill over the northern polar region in boreal winter. *Journal of Climate*, *33*(5), 1935–1951. https://doi.org/10.1175/JCLI-D-19-0408.1

Lorenz, E. (2006). Predictability—A problem partly solved. In T. Palmer & R. Hagedorn (Eds.), *Predictability of weather and climate* (pp. 40–58). Cambridge University Press.

Madden, R. A., & Julian, P. R. (1972). Description of global-scale circulation cells in the tropics with a 40–50 day period. *Journal of the Atmospheric Sciences*, *29*(6), 1109–1123. https://doi.org/10.1175/1520-0469(1972)029<1109:dogscc>2.0.co;2

Mallet, P. E., Claud, C., Cassou, C., Noer, G., & Kodera, K. (2013). Polar lows over the Nordic and Labrador Seas: Synoptic circulation patterns and associations with North Atlantic-Europe wintertime weather regimes. *Journal of Geophysical Research: Atmospheres*, *118*(6), 2455–2472. https://doi.org/10.1002/jgrd.50246

Miller, D. E., Wang, Z., Trapp, R. J., & Harnos, D. S. (2020). Hybrid prediction of weekly tornado activity out to Week 3: Utilizing weather regimes. *Geophysical Research Letters*, *47*(9). https://doi.org/10.1029/2020gl087253

Moreno-Ibáñez, M., Laprise, R., & Gachon, P. (2021). Recent advances in polar low research: Current knowledge, challenges and future perspectives. *Tellus A: Dynamic Meteorology and Oceanography*, *73*(1), 1–31. https://doi.org/10.1080/16000870.2021.1890412

Müller, M., Batrak, Y., Kristiansen, J., Køltzow, M. A. Ø., Noer, G., & Korosov, A. (2017). Characteristics of a convective-scale weather forecasting system for the European Arctic. *Monthly Weather Review*, *145*(12), 4771–4787. https://doi.org/10.1175/mwr-d-17-0194.1

Rasmussen, E. A., & Turner, J. (Eds.). (2003). *Polar lows: Mesoscale weather systems in the polar regions*. Cambridge University Press.

Rojo, M., Claud, C., Noer, G., & Carleton, A. M. (2019). In situ measurements of surface winds, waves, and sea state in polar lows over the North Atlantic. *Journal of Geophysical Research: Atmospheres*, *124*(2), 700–718. https://doi.org/10.1029/2017jd028079

Smith, L. C., & Stephenson, S. R. (2013). New trans-Arctic shipping routes navigable by midcentury. *Proceedings of the National Academy of Sciences*, *110*(13), E1191–E1195. https://doi.org/10.1073/pnas.1214212110

Stoll, P. J. (2022). A global climatology of polar lows investigated for local differences and wind-shear environments. *Weather and Climate Dynamics*, *3*(2), 483–504. https://doi.org/10.5194/wcd-3-483-2022

Stoll, P. J., Valkonen, T. M., Graversen, R. G., & Noer, G. (2020). A well-observed polar low analysed with a regional and a global weather-prediction model. *Quarterly Journal of the Royal Meteorological Society*, *146*(729), 1740–1767. https://doi.org/10.1002/qj.3764

Vitart, F., Alonso-Balmaseda, M., Ferranti, L., Benedetti, A., Balan-Sarojini, B., Tietsche, S., et al. (2019). *Extended-range prediction*. European Centre for Medium-Range Weather Forecasts.

Vitart, F., Ardilouze, C., Bonet, A., Brookshaw, A., Chen, M., Codorean, C., et al. (2017). The subseasonal to seasonal (S2S) prediction project database. *Bulletin of the American Meteorological Society*, *98*(1), 163–173. https://doi.org/10.1175/bams-d-16-0017.1

Vitart, F., & Miadek, R. (2021). ECMWF model—S2S—ECMWF confluence Wiki. Retrieved from https://confluence.ecmwf.int/display/S2S/ECMWF+Model

Wang, Z., Boyd, K., & Walsh, J. E. (2023). Modulation of polar low activity by the Madden-Julian Oscillation. *Geophysical Research Letters*. https://doi.org/10.1029/2023GL103719

Watanabe, S.-I. I., Niino, H., & Yanase, W. (2016). Climatology of polar mesocyclones over the Sea of Japan using a new objective tracking method. *Monthly Weather Review*, *144*(7), 2503–2515. https://doi.org/10.1175/mwr-d-15-0349.1

Wheeler, M. C., & Hendon, H. H. (2004). An all-season real-time multivariate MJO index: Development of an index for monitoring and prediction. *Monthly Weather Review*, *132*(8), 1917–1932. https://doi.org/10.1175/1520-0493(2004)132<1917:aarmmi>2.0.co;2

Wilks, D. S. (2011). *Statistical methods in the atmospheric sciences* (3rd ed.). Elsevier, Inc.

Zappa, G., Shaffrey, L., & Hodges, K. (2014). Can polar lows be objectively identified and tracked in the ECMWF operational analysis and the ERA-Interim reanalysis? *Monthly Weather Review*, *142*(8), 2596–2608. https://doi.org/10.1175/MWR-D-14-00064.1